ELSEVIER

Journal of Photochemistry and Photobiology A: Chemistry 119 (1998) 151–164

Journal of Photochemistry and Photobiology A:Chemistry

Degradation of naphthalene-1,5-disulphonate in a flow reactor. Modelling via reduced dimensionless centered variables

E. Balanosky[a], A. Lopez[b], J. Kiwi[a,*]

[a] *Institute of Physical Chemistry II, Swiss Federal Institute of Technology (EPFL), Lausanne 1015, Switzerland*

[b] *IRSA, Water Research Institute, Department of Water Chemistry and Technology, Experimental Laboratory, 20123 Bari, Italy*

Received 11 August 1998; accepted 14 September 1998

Abstract

This paper reports on a cylindrical concentric photochemical immersion-type reactor capable of degrading naphthalene 1,5-disulphonate, a non-biodegradable pollutant in the Rhine river. This study reports on the influence of the chemical parameters affecting the degradation, mixing conditions and processes taking place in the liquid being continuously replaced near the light source. A process mediated by Cu^{2+} / Fe^{2+} ions analogous to the Haber–Weiss cycle was found to be the system of choice for the substrate degradation. The optical absorption of the iron chromophore and not the intensity of the applied light was observed to be the most important factor determining the kinetics and efficiency during the degradation of the substrate. The degradation of the pollutant was studied in the 20–200 TOC (mg C l^{-1}) range. The photon flux of the actinic sources used varied between 0.8 and 3.1×10^{16} photons s^{-1} cm^{-2}. Experimental evidence is provided to the effect that no saturation effects were observed during reactor operation taking into account the concentration of the absorbing chromophore and photon flux in the reactor during the degradation experiments. The reactor volume of the mixing flask unit used was 2.33. The solution parameters used during flow mode operation made use of the experimental data found during the optimization of reactor batch mode operation. A single exponential function was constructed for the treatment of the experimental data to optimize the most economical use of chemicals, electrical energy and time to degrade a given amount of pollutant. This function allowed to predict the TOC values taking into consideration five of the chemical parameters affecting the degradation by way of reduced centered dimensionless variables. These variables significantly contributing to substrate degradation have been identified and modeled through contour plots and surfaces in two and three dimensions (2D, 3D). The abatement of the pollutant up to almost complete disappearance of the substrate was susceptible to modelization. The correlation factor between experimental and values predicted by the exponential function was better than 95% as computed by the appropriate analytical function. The sulfo-groups play an important role in the recalcitrance of naphthalene 1,5-disulphonate. These sulfo-groups are seen to be rapidly removed by the pretreatment used allowing the substrate to reach biocompatibility in a few minutes.

Keywords: Fenton photo-assisted reaction; Exponential modeling; Photocatalysis; Solution parameters; Biodegradation

1. Introduction

Aromatic sulphonates are typical components of industrial waste waters which play a particular role in the overloading of the Rhine river [1,2]. Aromatic sulphonates are widely used in dye-stuff production, as intermediates in ion exchange resins, plasticisers, pharmaceuticals and are commonly found in effluents of the textile industry. They are hydrophilic substances with limited biological degradability as in the case of naphthalene 1,5-disulphonic acid disodium salt (from now on Naph-Dis). Therefore, these substances appear as residues from industrial processes in biologically treated waste waters in general [3,4] and in the Rhine river in particular. Since Naph-Dis is soluble in water and have xenobiotic character their appearance in drinking water should be avoided.

Naphthalene-sulphonic compounds have been reported to decrease the pH and biological activity of the microflora in water estuaries [5,6]. Adapted bacterial sludge has been used over prolonged time periods on Naph-Dis with modest degradation rates indicating the recalcitrant nature of this residue material [4,7–9]. Consequently, pretreatment and elimination of Naph-Dis have been attempted by adsorption on activated carbon [10] but this method is costly since it is followed by membrane filtration (Siran). Treating with O_3 [11] was effective in reducing about 60–70% of Naph-Dis independent of pH and initial substrate concentration. But a high level of O_3 was necessary to reach good biodegrad-

*Corresponding author. Fax: +41-21-69-34-111.

1010-6030/98/$ – see front matter
PII: S1010-6030(98)00399-2

ability (BOD_5 / COD = 0.4, BOD_5 being the amount of oxygen utilized when the organic matter in a given volume of water is degraded biologically). About 3.5 mg of O_3 were necessary per 1 mg initial DOC substrate. Naph-Dis have been reported to be oxidized by hypochlorite but the latter treatment leads to toxic chlorinated compounds in the water supply due to the formation of chlorinated by-products [12]. A reliable quantitative evaluation of the biodegradability of aromatic sulphonates is complicated by the fact of the simultaneous volatilization and adsorption of these compounds into the biomass [1–6]. The sulfo-substituent on naphthalene decreases the electronic density of the aromatic ring and deactivates the rings with respect to electrophilic attack by the OH· radical increasing the resistance to bacterial degradation [13].

Light-induced methods for the removal of pollutants have been shown to be possible and of applied interest [14,15] when the light absorption in the system used is adequate. Recent work with photoreactors in this area has only been explored in a few studies and not much engineering work has been devoted to this subject [16,17]. Modeling of such devices in homogenous systems in photoreactors using Fenton systems is only at the beginning stage as a part of the recent developments taking place in the field of advanced oxidation technologies [18,19].

In this work the modeling by way of a simple mathematical exponential polynomial for the treatment of experimental data allowed to predict the optimal region(s) for the lower final TOC. In other words, the better combination of chemical parameters to be used during the degradation of the Naph-Dis and intermediates was found by a rigorous approach and not by successive experimental optimization as has been done until now [3,5,14,18,19].

2. Experimental

2.1. Materials

Naph-Dis was product of EMS-Chemie (No. 60499 with 5% NaCl). Mohr's salt (ammonium ferrous sulfate hexahydrate), $CuSO_4 \cdot 5H_2O$ and H_2O_2 (30% w / w) were Fluka p.a. and used as received. The Fe^{3+} and Cu^{2+} ions were added at the beginning of each run. The consumption of H_2O_2 during the reaction was followed by the Merckoquant® test for peroxides which detected peroxides between 0.4 and 25 mg l^{-1}. Solutions of Naph-Dis were acidified to the desired pH with 1 M H_2SO_4.

2.2. Reactor

A Philips 36 W (1.20 m long and 26 mm in diameter, TLD 36 W / 08) black actinic light source was employed in such a way that its center passed through the focal axis of the immersion-type reactor having 35 mm diameter. A scheme for the reactor set-up is shown in Fig. 1. The lamp radiation was centered at 366 nm with a λ-distribution between 330 and 390 nm. A 140 W Philips lamp with the same λ-distribution but 140 W power (140 W / 05) was used to compare the effect of the variation of light intensity on the degradation rate. A third lamp with a different light distribution (TL 40W / 03) and a λ-distribution from 390 to 480 nm and centered around $\lambda = 435$ nm was also used to test the effect of light distribution during the degradation process. The reactor mixing flask had a 1 l volume equal to the volume of solution used in the batch mode experiments. The reactor volume was 1800 ml and the volume of the tubing (Fig. 1) was 306 ml. The volume of the reactor to the volume of the mixing flask was 2.33. During flow through experiments the Naph-Dis solution was fed into a system from the 20 l reservoir and H_2O_2 was added by means of a peristaltic pump into the 1 l mixing flask.

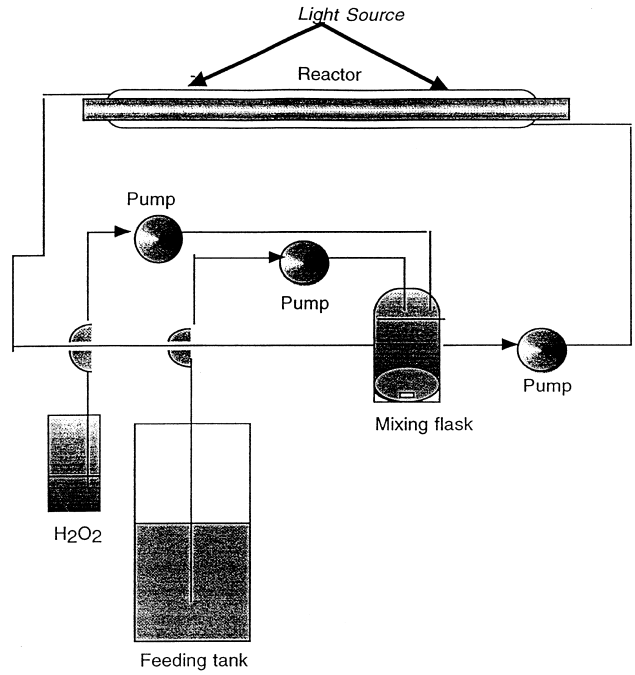

Fig. 1. Schematic of the photoreactor setup (a) batch reactor mode operation. The feeding tank was not part of the experimental setup and (b) when larger volumes of solution to be treated in flow reaction operation mode the 20 l tank becomes a part of the unit. For further details see text.

2.3. Analysis in solution

Total organic carbon (TOC) was monitored during this study with a Shimadzu 500 provided with an automatic autosampler. High pressure liquid chromatography (HPLC) was carried out with a Varian 9100 LC unit equipped with a 9065 diode array. The column used was a Spherisorb ODS-2 5 mm and the mobile phase consisted of a ammonium acetate solution in an acetonitrile–water solvent. The ammonium acetate was 0.3 M at zero time. At 20 min the mobile phase was 70% ammonium acetate and 30% acetonitrile. After 30 min, the mobile phase consisted of 100% ammonium acetate. The peak of Naph-Dis was observed after ~14 min. Spectrophotometric measurements were carried

out with a Hewlett–Packard 386 / 20 N diode array. The presence of sulfates in the solution was detected by ion-liquid chromatography (ICL) with a Dionex ion analyzer provided with a Hamilton PRPX-100 anion column and a mobile phase consisting of 2 mM phthalic acid at pH 5.

2.4. Test of bacterial activity

Biological oxygen demand (BOD_5) was carried out on pretreated and non-treated solutions in the dark, at room temperature for 5 days by means of a Hg-free WTW 2000 Oxytop unit thermostated at 20°C. At 20% inoculum, the volume of the bacterial solution in reaction to the volume of the total BOD sample taken was used. To this solution phosphate buffer and the necessary nutrients, salts and trace elements were added [4].

3. Results and discussion

3.1. Dark degradation runs with Fenton systems: Reactor batch mode operation

Fig. 2 presents the results for the degradation in the dark of Naph-Dis adding: (a) $Fe^{3+} + H_2O_2$, (b) $Cu^{2+} + H_2O_2$ and the combination of both cations equimolar quantities in the presence of H_2O_2 (pH 2.8). After the preliminary optimization experiments it was seen that the effect of the Fenton-like systems increase in the order Fe^{3+}, Cu^{2+} and $Fe^{3+} + Cu^{2+}$. The traditional Fe ion-based Fenton systems have been reported extensively in the literature [3,20,21]. The Cu ion-catalyzed systems have recently been reported by work out of our laboratory [22,23] and are seen to be more effective in catalyzing the substrate degradation in

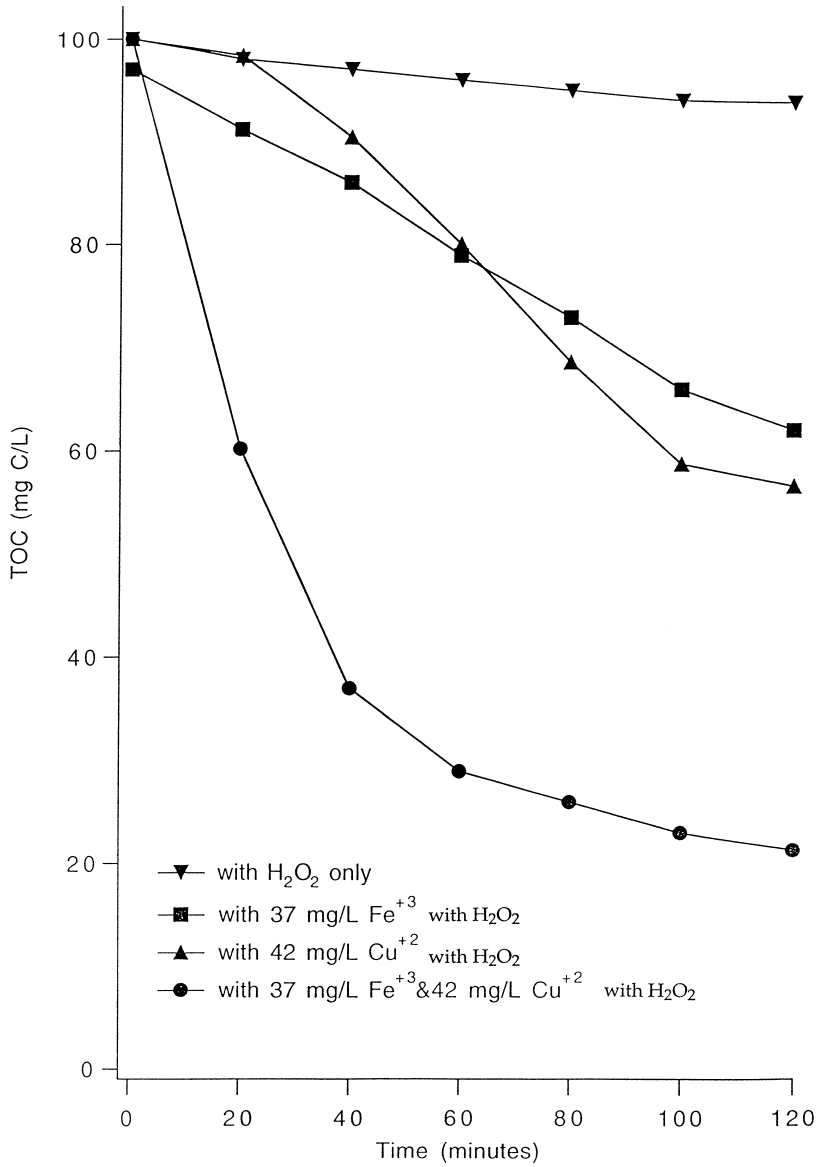

Fig. 2. Dark reactor degradation of Naph-Dis (0.79 mM) as a function of time in the presence of H_2O_2, Fe^{3+} and Cu^{2+} ions in the quantities mentioned in the caption to the Figure.

combination with Fe-ions. In Fig. 2, oxidation of Naph-Dis in the dark is seen to be negligible when only H_2O_2 was added. The $Fe^{3+} + Cu^{2+}$ combination of ions was seen to be the most active system to catalyze the peroxide decomposition in the dark. The details of the latter process will be discussed in Section 3.3.

The dependence of Naph-Dis degradation on the amount of added H_2O_2 is shown in Fig. 3. Lower rates of oxidant addition were observed to be adequate to induce a kinetically fast degradation of the substrate. A degradation of $90 \pm 4\%$ was attained in ~20 min for an oxidant addition rate of 150 μl min^{-1} l^{-1}. This is the amount of H_2O_2 added directly per litre of solution to be treated in the mixing flask shown in Fig. 1. Higher rates of oxidant addition in Fig. 3 did not lead to higher degradation rates. This is seen by the run using 300 μl min^{-1} l^{-1} H_2O_2. It is known after the initiation steps (Eqs. (3), (4) and (5))

$$H_2O_2 + Fe^{2+} \rightarrow Fe^{3+} + OH^- + OH\cdot$$
$$E^\circ = 0.74\,(\text{V NHE, pH 0}) \quad (1)$$

the propagation step in Eq. (2) would be hindered by excess of H_2O_2 acting as OH· scavenger for the radicals in solution

$$H_2O_2 + OH\cdot \rightarrow H_2O + HO_2\cdot \quad E^\circ = 0\,(\text{radical reaction}) \quad (2)$$

The inset in Fig. 3 shows a reduction of the absorbance during of 68% at $\lambda = 366$ nm within a 2 h period. The inset in Fig. 3 shows the absorbance at time zero ($A = 1.5$) taken at $\lambda = 366$ increasing initially ~10–15% within 20 min. This is possible due to the build-up solution intermediates. Subsequently a decrease in absorbance is observed down to $A = 0.6$. The optical transmission of the solution increased by ~73% within 2 h. The observed absorption at $\lambda = 366$ at time zero is exclusively due to the Fe^{3+} aqua complexes in the solution (see the inset to Fig. 5). It is followed by a decrease in the optical absorption with time due to: (a) the mineralization of the organic intermediates as shown by the TOC values in Fig. 3 and (b) the decrease of the initial concentration of the Fe(III)–aqua complex in solution

$$Fe(III)_{aq} + H_2O_2 + H_2O \rightarrow Fe(II)_{aq} + HO_2\cdot + H_3O^+$$
$$E^\circ = 0.67\,(\text{V NHE, pH 0}) \quad (3)$$

While the $Fe(III)_{aq}$ complexes in acid solution: $Fe(OH)^{2+}$ with $\varepsilon_{366\ nm} = 275\ M^{-1}\,cm^{-1}$ [24] and $Fe(OH)_2{}^{4+}$ with $\varepsilon_{366\ nm} = 1000\ M^{-1}\,cm^{-1}$ [25] decrease in concentration after the beginning of the reaction. But the absorption of Fe(II) increases during the reaction due to absorption of the $Fe(H_2O)_6{}^{2+}$ charge transfer band. This band does not absorb at $\lambda = 366$ nm. Its absorption begins at $\lambda = 265$ nm with $\varepsilon_{254\ nm} = 20\ M^{-1}\,cm^{-1}$ [26]. The build-up of Fe^{2+} ionic species in solution takes place at the expense of the Fe^{3+} ion in the solution. In Fenton systems iron Fe^{3+} and Fe^{2+} are known to coexist in solution [3–5,21–23].

High pressure liquid chromatography (HPLC) was performed along the TOC measurements during the degradation shown in Fig. 3. The Naph-Dis was observed to elute at about 10 min in the HPLC chromatogram. But the disappearance of Naph-Dis was observed to take place below 10 min creating an additional complication in the determination of the Naph-Dis by HPLC. The identification of the Naph-Dis was also complicated by relatively high amounts of Fe ions in the solution. Better defined peaks in the spectrogram were observed in the presence of lower Fe concentrations in the solution. This is why the disappearance of Naph-Dis is not shown in Fig. 3. Throughout this work, TOC measurements were therefore used to measure the degradation of Naph-Dis.

3.2. Degradation of Naph-Dis as a function of recirculation rate, substrate concentration and light source during reactor batch mode operation

Fig. 4 shows the reduction in TOC of the solution with time indicating a flow beyond 270 ml min^{-1}, a faster recirculation of the solution in the reactor will not accelerate the degradation kinetics. The run with a recirculation rate of 120 ml min^{-1} is seen to be less efficient during reactor batch mode operation. The volume of the reactor where the solution undergoes light irradiation is much less than the total volume to be treated during the reactor operation. This is shown in Fig. 1. At any time during the operation more than 75% of the solution to be treated was in the dark and less than 25% underwent light irradiation. When the recirculation rate increases from 120 to 270 ml min^{-1}, the recirculation rate increases and mixing in the whole system is improved leading to an increase in the reaction rate up to 270 ml min^{-1} (in Fig. 4). Beyond this value, no further acceleration of the degradation kinetics was observed. In other words, we have attained the limit for the degradation proceeding at a constant rate k.

The inset to Fig. 4 shows the photodegradation of Naph-Dis as a function of substrate concentration. The Naph-Dis degradation resembles a decay process with first-order kinetics

$$C(t) = C_0 \exp(-kt) \quad (4)$$

It is interesting to note that the degradation of the substrate proceeds efficiently within a 2 h period even for relatively concentrated Naph-Dis solutions up to 0.525 g l^{-1} or 1.58 mM. The increasing optical absorption of the higher substrate concentrations does play a determining role during the degradation. The Fe^{3+} band acting as the active chromophore in the solution determines the absorption of light in the system. In presence of H_2O_2 the excitation of the Fe^{3+} charge transfer band gives rise to the radicals leading to the abatement of Naph-Dis [14–19,22,23].

Fig. 5 presents the degradation of Naph-Dis in the reactor using (a) a 36 W Philips actinic light source with $\lambda_{max} = 366$ nm as in Figs. 2–6, (b) a 140 W Philips actinic

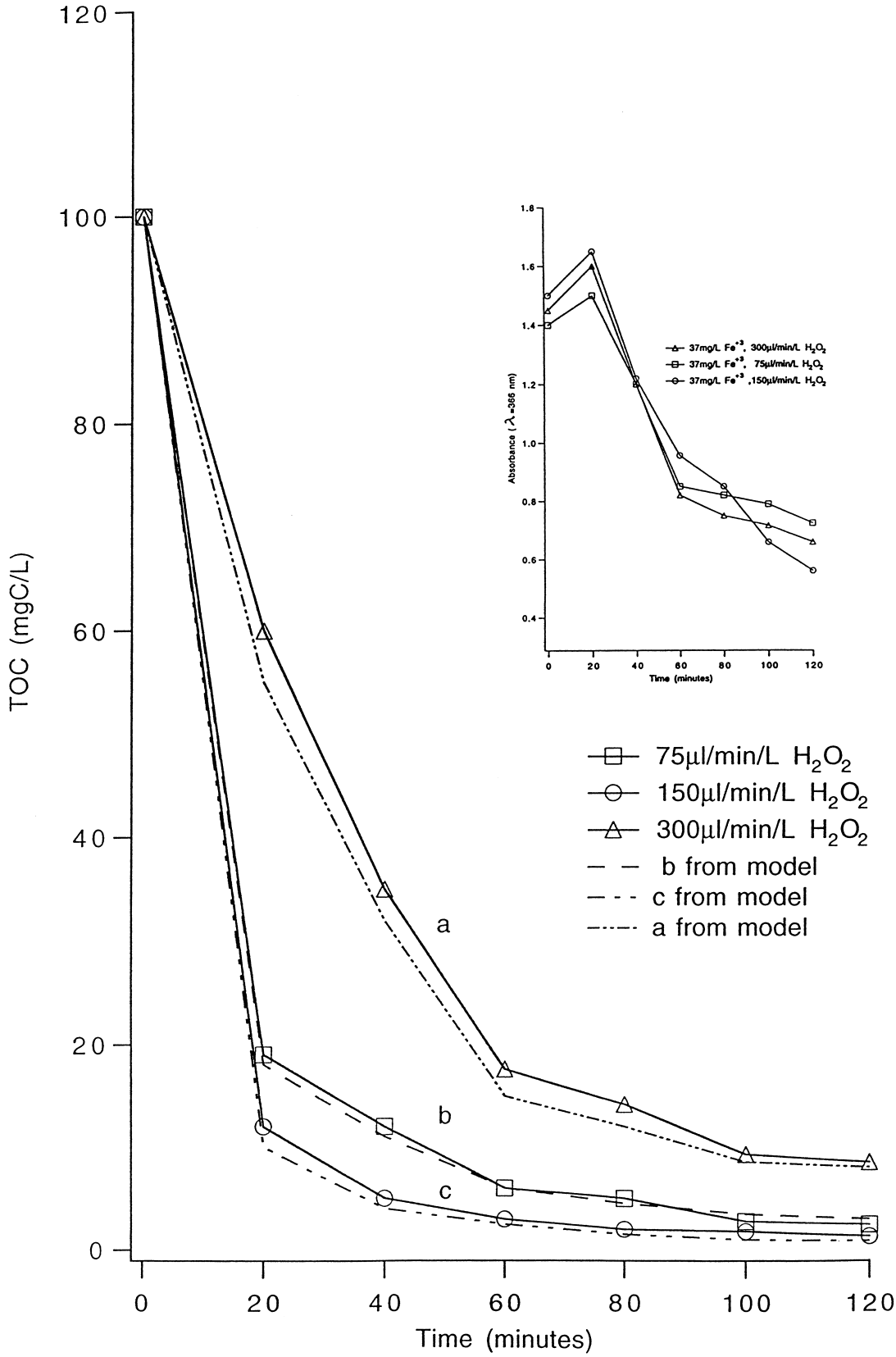

Fig. 3. Reactor degradation of Naph-Dis (0.79 mM) in the presence of Fe^{3+} (37 mg l^{-1}) as a function of time under irradiation of a 36 W actinic lamp. The amount of H_2O_2 varies during the reactor batch mode operation (see Figure caption). The inset shows the decrease in absorbance (A) as a function of time for this run at $\lambda = 366$ nm.

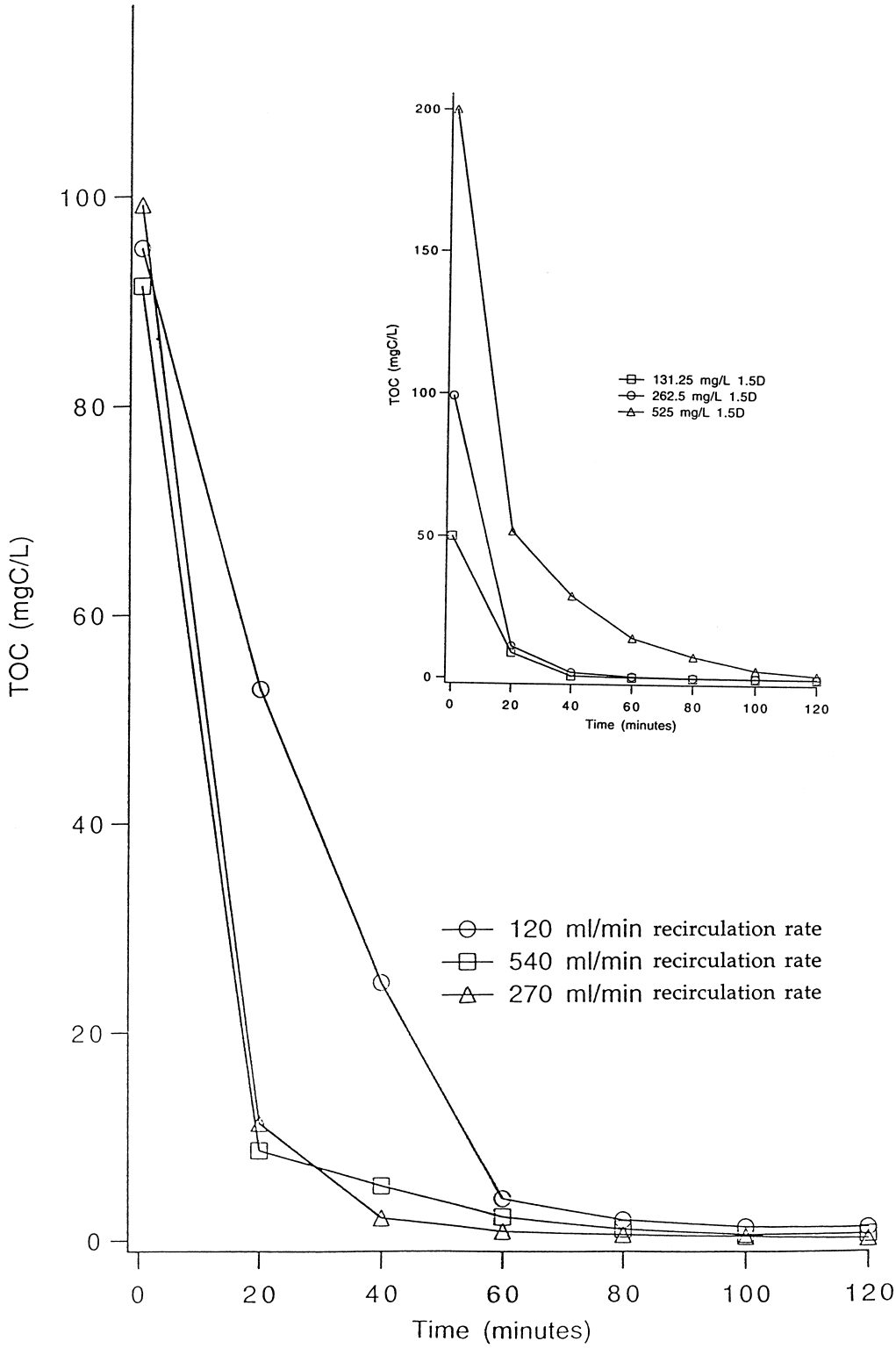

Fig. 4. Reactor degradation of a Naph-Dis (0.79 mM) in the presence of Fe^{3+} (37 mg l^{-1})/Cu^{2+} (42 mg l^{-1}) and 150 μl min^{-1} l^{-1} H_2O_2 as a function of time. The recirculation rate of the solution in the reactor is shown in the figure caption. The inset shows the photodegradation for different concentrations of Naph-Dis solutions in the presence of Fe^{3+}(37 mg l^{-1}) / Cu^{2+} (42 mg l^{-1}) and 150 μl min^{-1} l^{-1} H_2O_2. Actinic light irradiation under (36 W) is used.

light source with the same dimensions and λ_{max} as in (a) and finally (c) a Philips visible light source (40 W) centered with $\lambda_{max} = 435$ nm (see Section 2). The results obtained in Fig. 5 show that the increase in light intensity did not accelerate the observed degradation kinetics or efficiency. These results can only be understood in terms of the Fe^{3+} ion

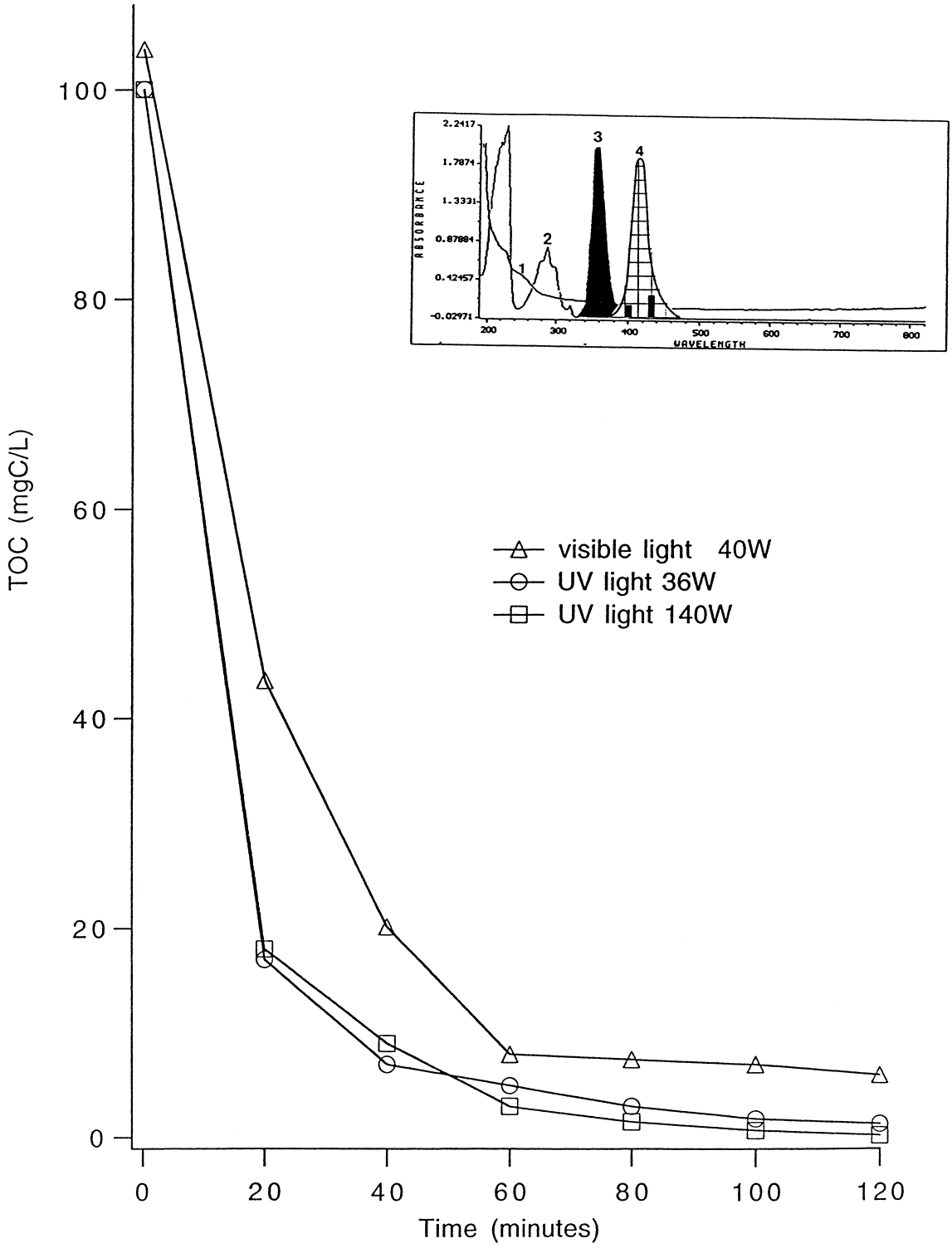

Fig. 5. Reactor degradation of a Naph-Dis (0.79 mM) in the presence of Fe^{3+} (37 mg l^{-1}) Cu^{2+} / (42 mg l^{-1}) and 150 μl min^{-1} l^{-1} H_2O_2 as a function of time. The recirculation rate flow used was 270 ml min^{-1}. The intensities and type of light source are noted in the figure caption. The inset shows: (1) the absorption of Fe^{3+} ion at pH 2.8, (2) the absorption of Naph-Dis and (3) the relative spectral power distribution as a function of λ for the 36 W actinic lamp (4) the same as in (3) but for the lamp centered at 435 nm.

being the active chromophore absorbing the light irradiation in the chemical system. The optical absorption of Fe-species between 330 and 390 nm is a determinant for the absorption of the complete system Naph-Dis / Fe^{3+} + Cu^{2+} / H_2O_2 in the reactor since (a) both actinic lights induce similar degradation kinetics indicating that the degradation process

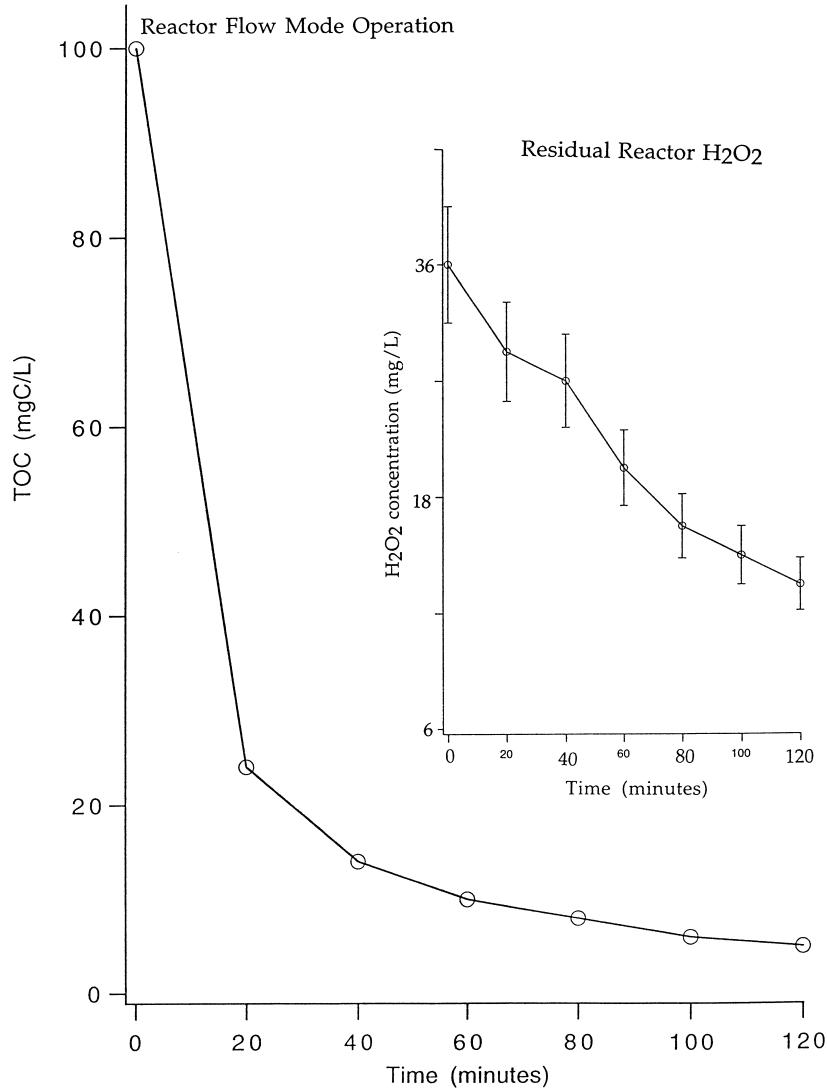

Fig. 6. Reactor flow mode operation observed during degradation of Naph-Dis (0.79 mM) with Fe^{3+} (37 mg l^{-1}) / Cu2 + (42 mg l^{-1}) and 150 μl min^{-1} l^{-1} H_2O_2 under actinic light irradiation (36 W). The 20 l Naph-Dis solution was made available from the feeding tank (see Fig. 1). The inset shows the residual H_2O_2 in the reactor during this flow run.

does not depend on the intensity of the light source used but on the amount of light being absorbed by the chromophore, namely the Fe^{3+} species. The solution in Fig. 5 contains 37 mg l^{-1} of Fe or 0.66 mmoles of Fe l^{-1}. Taking into account the 1636 cm^2 illuminated reactor surface there are 2.5×10^{18} molecules Fe ions cm^{-2}. The 36 W actinic light has a photon flux of 0.8×10^{15} photons s^{-1} cm^{-2} and 140 W actinic light source (Fig. 5) had a photon flux of 3×10^{16} photons s^{-1} cm^{-2}. In both cases we are well below the saturation value for the Fe^{3+} ion which is the only absorbing species in the solution. No saturation effects in the conventional sense can be responsible for the lack of increase in the degradation kinetics of Naph-Dis when 140 W lamp is used compared to the 36 W (Fig. 5). This can be rationalized by a slower rate of disappearance of the excited state $Fe(H_2O)^{3+*}$ in solution in relation to the rate of production or creation of these excited states due to light irradiation. These excited states have a lifetime with an upper limit of 10^{-8} s [3,18,22] but it is not possible to measure in these extremely short time domain the rate constants for the creation of the excited states, the radiation transition for the deactivation from the excited state as separate effects and directly the lifetime of the excited state which is a function of the solution components and the intensity of the applied light. (b) The Cu^{2+} ions, H_2O_2 and Naph-Dis added did not absorb in the range of the light source, (c) when a visible light source centered at $\lambda = 435$ nm was used, a less efficient degradation of Naph-Dis was observed. This is due to the lower absorption of the Fe-species at longer wavelengths since the latter light source emits predominantly in the visible region. The inset in Fig. 5 shows the relative spectral power distribution of the two lamps used for the runs shown in Fig. 5. Trace 3 presents the actinic lamp centered at 366 nm and trace 4 in the inset

presents the distribution for the lamp centered at $\lambda =$ 435 nm. In the latter case the 2 Hg resonance lines are shown within the emission boundaries, (d) Fig. 4 (inset) did not present marked changes for the TOC reduction rate in spite of significant variation of the concentration in Naph-Dis and finally (e) the concentrations of the iron used allow an absorbance $A = 1.20$ where 94% of the total incident photon flux is absorbed by the solution.

3.3. Reactor flow mode operation experiments: Quantitative assessment of H_2O_2 during degradation of Naph-Dis

During reactor flow mode operation the intention was to degrade a larger amount of the initial substrate (20 l) being slowly added via a peristaltic pump from the feeding tank (see Fig. 1) to the mixing flask while at the same time the reactor solution is being recirculated in the reactor with a rate at 120 ml min^{-1}. The latter recirculation rate during the flow mode operation was selected after preliminary optimization experiments. Its value is seen to be lower than the recirculation rate previously used during the reactor batch mode operation. During reactor flow mode operation the degradation of 20 l of Naph-Dis within a 2 h period is presented in Fig. 6. Optimal degradation during flow experiments were observed with 120 ml min^{-1} (7.2 l h^{-1}) or a residence time was 0.138 h. In a typical flow experiment as reported in Fig. 6, the solution of Naph-Dis (0.79 mM) with Fe^{3+} (37 mg l^{-1}) + Cu^{2+} (42 mg l^{-1}) adding 150 μl min^{-1} l^{-1} H_2O_2 recirculates at a flow of 120 ml min^{-1}. The Naph-Dis solution is carried from the feeding tank (20 l) to the photoreactor within 2 h period. Concomitantly recirculation of this solution goes on the set-up shown in Fig. 1 where the H_2O_2 is dosed into the 1 l mixing flask. This latter operation is carried out by means of a peristaltic pump. Therefore, we need (a) a pump to recirculate the solution from the mixing flask trough the photoreactor, (b) a second peristaltic pump to add H_2O_2 during degradation and (c) a third peristaltic pump to carry the 20 l Naph-Dis to the photoreactor during flow experiments. The results shown in Fig. 6 are encouraging since they allow to treat a relatively large volume of Naph-Dis solution (~0.24 m^3 / 24 h) with a low electrical power actinic light. From Fig. 6, the kilowatt-hours necessary to reduce the concentration of 1 m^3 Naph-Dis by one order of magnitude is ~2.4 kWh m^{-3}/order [19]. This takes into account that the time required to reduce 90% of the initial solution C-content (Fig. 6) is about 80 min for the 20 l Naph-Dis available in the feeding tank.

The input concentration as seen from Fig. 6 is 100 mg C l^{-1}. The feeding rate used was of 1000 mg C l^{-1} h^{-1} and the observed output concentration was 7 mg C l^{-1} of TOC. The degradation rate was therefore 496 mg C l^{-1} h^{-1}. The concentration of H_2O_2 was followed by the Merckoquant® paper in mg l^{-1} (see Section 2). The results are shown in the inset of Fig. 6. The oxidation level in solution is seen to decrease as the reaction progresses. Mineralization of 93% (Fig. 6) of the initial TOC occurs consuming ~64% of the initial H_2O_2 after 2 h (inset of Fig. 6). This experiment was not designed for the total elimination of the residual oxidant within the pretreatment period. The 150 μl min^{-1} l^{-1} or 0.15 ml min^{-1} l^{-1} is equivalent to the addition of 36 mg H_2O_2 after instant zero into the 1.4 mixing flask. Since the H_2O_2 used was 30% by weight then 50 mg H_2O_2 are added / 1.4 l or 36 mg H_2O_2 l^{-1} as shown in the inset to Fig. 6.

The optical density of the solution was also followed during the reactor flow operation. A decrease from $A = 1.5$ to ~0.3 (path length = 1 cm) was observed for the optical absorption at $\lambda = 366$ nm within 2 h. Within a 4 h period the oxidation of a solution containing 15.8 mmoles Naph-Dis was seen to require 310 mmoles of H_2O_2. This result is consistent with a 97% reduction of the initial substrate (within the 4 h period). The oxidant-to-pollutant ratio of 19.6 found suggested the approximate mineralization stoichiometry

$$C_{10}H_6Na_2O_6S_2 + 20H_2O_2 + 4H_2O \rightarrow 10CO_2 + 22H_2O + 2Na^+ + 2SO_4^- + 2H^+ \quad (5)$$

During the flow experiments Cu^{2+} was used in addition to Fe^{2+} as a photocatalyst in the presence of H_2O_2. Dark experiments in Fig. 1 (trace 4) indicated than when these two ions are added in solution, more efficient TOC reduction was observed than when either Cu^{2+} or Fe^{2+} ions were added separately. Figs. 3–6 have shown results for Naph-Dis abatement in a cycle analogous to the Haber–Weiss [27] when adding the two ions mentioned above into the solution. Cu^{2+} is a more energetic oxidant than the Fe-ion for the H_2O_2 present when comparing the reduction potential in solution since reaction (Eq. (6))

$$Cu^{2+} + H_2O_2 \rightarrow Cu^{1+} + HO_2\cdot + H^+ \quad (6)$$

involves two couples with the potential Cu^{2+} / Cu^{+1} (0.16 V) and $H_2O_2/HO_2\cdot$, H^+ (1.44 V) rendering a potential for reaction (Eq. (6)) of 1.28 V NHE. This potential is higher than in the reaction Fe^{3+} / Fe^{2+} with H_2O_2 (see reaction (Eq. (3))). From the couples Fe^{3+} / Fe^{2+} (0.77 V NHE) and $H_2O_2/HO_2\cdot$, H^+ (1.44 V NHE) the combined potential is 0.67 V NHE. The Cu^+ (from Eq. (6)) additionally produce more OH· radical in solutions

$$Cu^{1+} + H_2O_2 \rightarrow Cu^{2+} + OH\cdot + OH^- \quad (7)$$

If RH represents Naph-Dis, then the reactions (Eqs. (11)–(13)) can occur involving Cu^{2+} with Fe^{2+} ions in the presence of the organic molecules

$$OH\cdot + RH \rightarrow R\cdot + H_2O \quad (8)$$

$$R\cdot + Cu^{2+} \rightarrow R^+ + Cu^{1+} \quad (9)$$

$$R\cdot + Fe^{2+} \rightarrow R^+ + Fe^{3+} \quad (10)$$

$$Cu^+ + Fe^{3+} \rightarrow Cu^{2+} + Fe^{2+} \quad (11)$$

Eqs. (9) and (10) shows Cu^{2+} ions reacting with organic radicals [22,23] and subsequently reducing the Fe^{3+} with

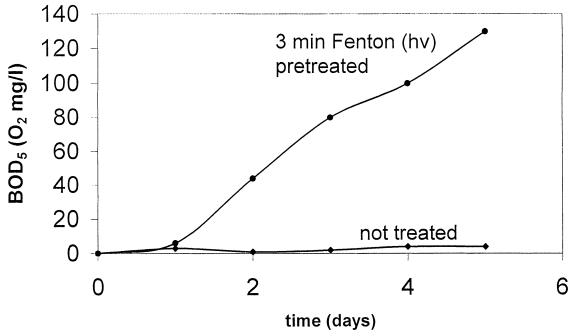

Fig. 7. Biological oxygen demand for pretreated and not treated solution of Naph-Dis. The pretreatment was carried out as in Fig. 5 using a 36 W actinic light source.

further generation of OH· radicals. The latter step accounts for the beneficial effect of Cu^{2+} ion addition accelerating the substrate degradation.

3.4. Biological oxygen demand and nature of the intermediates produced during the pretreatment

Fig. 7 shows the BOD_5 measurements for two solutions of Naph-Dis. Almost no increase in the 5 day period was observed for the non-treated substrate. But a solution containing 100 ppm C of substrate pretreated under light with Fe^{3+} / Cu^{2+} / H_2O_2 for 3 min showed a steep rise after 1 day for the BOD_5 values. Pretreatment times were no longer necessary since fast biodegradation rates were already induced after this short pretreatment period. Water sewage was taken after a primary decantation process of the Vidy (VD), Switzerland waste-water treatment plant. This solution was further decanted for 24 h, filtered through cotton and used as an inoculum. A blank run was carried out with sewage bacteria only. The formula used to calculate the BOD reported in Fig. 7 is

$$\mathrm{BOD} = \frac{\mathrm{BOD\ measured} - 0.01\{\%\mathrm{inoculum} \times \mathrm{BOD\ inoculum}\}}{\{100 - \%\ \mathrm{inoculum}\} \times 0.01} \tag{12}$$

The results presented in Fig. 7 suggests that other non-biodegradable intermediates besides Naph-Dis are also removed during the short pretreatment due to the steep rise observed for the BOD as a function of time. Fig. 7 also shows after 1 day the efficiency of bacterial action. This moved us to identify the nature of some of the more oxidizable intermediates by HPCL and by ILC (see Section 2 for further details).

In separate experiments by ICL the hydrolysis of Naph-Dis in a solution was seen to rapidly release sulfate ions during reactor flow operation. The photo-oxidation C–S bond fission leading to the release of sulfate ions was seen from the beginning of the reaction. The desulfonation proceeds upon OH· attack with simultaneous substitution of the sulfo-groups by hydroxy-groups in the naphthalene forming naphthalene-dihydrol [28].

Fig. 7 shows a rapid increase in the BOD_5 after 3 min pretreatment. The negative effects of the sulfo-groups due to their strong electronic withdrawing effects and other the steric effects affecting adversely the biodegradability of the substrate are remove within this short pretreatment time. The HPLC spectrogram identified naphthol isomers and isomers of naphtoquinone besides carboxy cinnamic and phthalic acids as being produced during the pretreatment period. The observed intermediates are in agreement with the work reported by Bahnemann and Atkinson [29,30] involving intermediates found during the catalytic and photocatalytic degradation of naphthalenes and naphthalene-sulphonates.

3.5. Mathematical modeling via exponential function of the degradation parameters in the flow reactor through dimensionless variables

It was experimentally observed that the TOC decrease with time (Figs. 2–6) followed an exponential decay. Therefore an exponential function was taken to fit the experimental results observed. This will be shown in a detailed way in Figs. 8–10.

Some years ago the methodology for building a statistically significant model was devised for a set of well chosen experiments [31]. This study addresses the problem of constructing a simple exponential function which fits the observed degradation data. Contour plots or curves of constant response value will be used to predict the value of the variable at any point in the region of interest [32]. This methodology has been applied to investigate and identify the main variables contributing to the degradation process: H_2O_2 concentration, Fe^{3+} ions, *p*-NTS concentration, recirculation flow or time of residence and intensity (I) of the light source. Recently out of our laboratory the degradation of *p*-nitrotoluensulfonate in a photoreactor was modeled by way of single polynomial expression [33].

The approach used during the present study takes the experimental data in pairs, X_1 and X_2 (reaction parameters). Each graph represents a set of 48 pair of values for TOC as a function of the five reaction parameters. Reduced-centered dimensionless variables of these parameters are worked out in order to avoid having different units for different variables. Each reduced centered variable X_i was specifically associated to a specific solution parameter u_i in such a way that $X_i = (u_i - u_{io})/\Delta u_i$, where: u_{io} is the value of u_i at the center of the experimental region and $\Delta u_i = (u_{i\max} - u_{i\min})/2$.

The treatment of the data takes the experimental data in pairs, X_1 and X_2 (reaction parameters). Each graph represents a set of 48 pairs of values for TOC as a function of the reaction parameters. Then a simple exponential expression can be constructed in the form of

$$Z = b_o \exp\left[s\left(\sum b_i X_i + \sum b_{ii} X_i^2 + \sum\sum b_{ij} X_i X_j\right)\right] \quad (13)$$

where, $b_o = \sum Z_i/N$ is the average of the values of TOC over N experimental points, b_i the coefficients for the main effect of the variable X_i and $b_i = \sum_i Z_i X_i/N$, b_{ii} the coefficients for the quadratic effect of the variable X_i and $b_{ii} = \sum_i Z_i X_i^2/N$, b_{ij} the coefficient for the first order interaction effect of X_i and X_j and $b_{ij} = \sum_i Z_i X_i X_j/N$, and s (scaling factor) is used to adjust the fitting of the curves for the initial and final concentrations of the reagents.

A set number of six experimental points is taken with eight TOC values corresponding to each of the values found for X_i, that is 48 values in total. In each case, the TOC values were multiplied by the values of the corresponding X_i. The 48 products found were added up and divided by 48 to find the coefficient for b_i. Coefficients noted by b_{ii}'s represent the quadratic effect. To find the b_{ii}'s value, each TOC value was multiplied by the square of the corresponding x_i, the 48 products were added up and divided by 48. To find the b_{ij} coefficients representing the first-order interaction effect between X_i and X_j, the TOC values found experimentally were multiplied by X_i and X_j and the 48 products added up and divided by 48. The values of the X_i variables were taken as follows.

Range of X_i (contour plots and 3D surfaces)

X_i	−1	−5 / 7	−3 / 7	−2 / 7	−1 / 7	−1 / 3	1 / 7	3 / 7	5 / 7	1
$[H_2O_2]$ (ml l^{-1})	0	3	6		9		12	15	18	21
[1.5 D] (mg l^{-1})	131.25					262.5				525
$[Fe^{3+}]$ (mg l^{-1})	18.5				37					75
Flow (ml min^{-1})	120			270						540

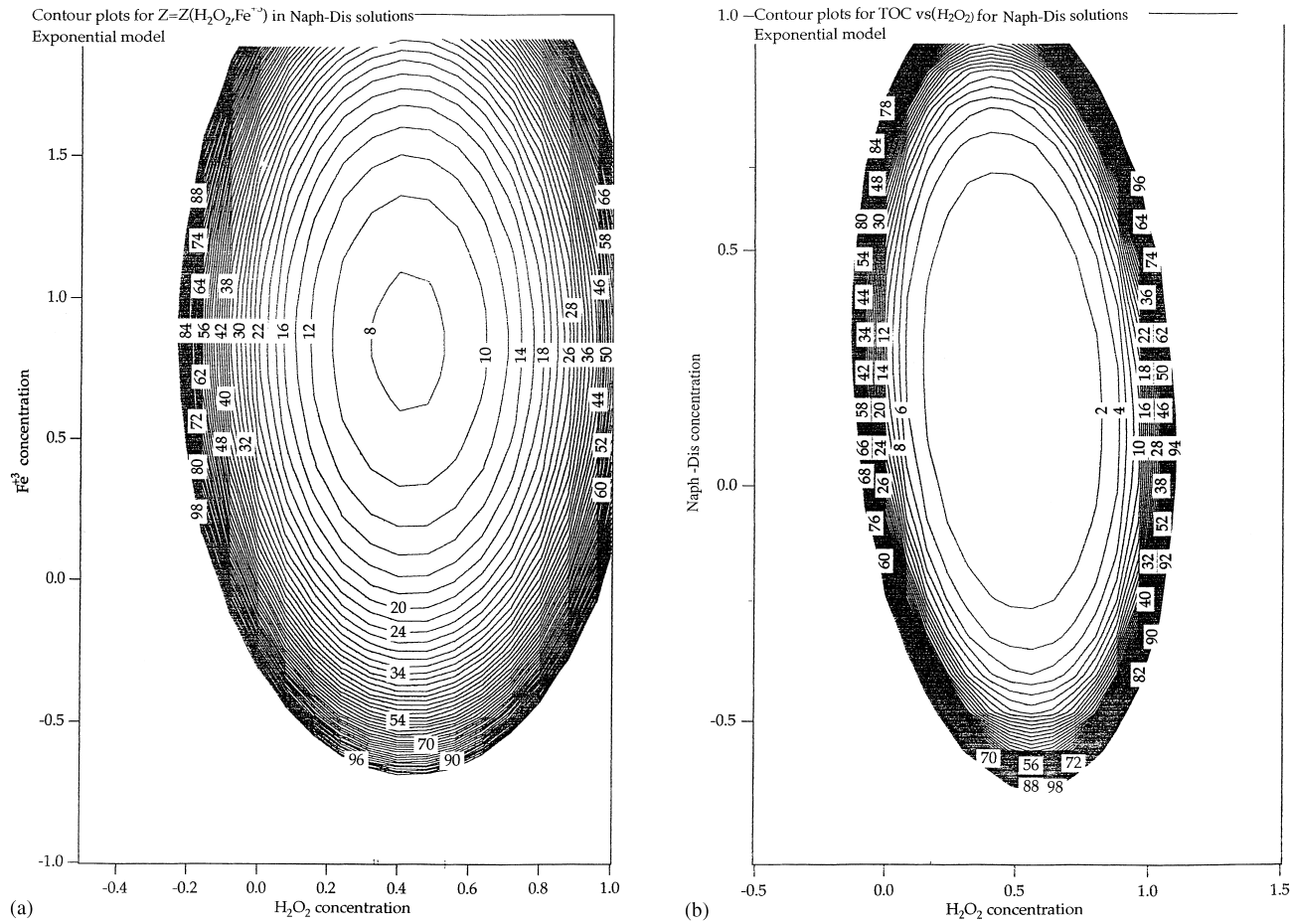

Fig. 8. 2D contour plots obtained from exponential function for the data reported in Figs. 3–6, for the pair of variables (a) Fe^{3+} and H_2O_2 (b) Naph-Dis and H_2O_2 (c) Naph-Dis and Fe^{3+} and (d) recirculation rate and Naph-Dis.

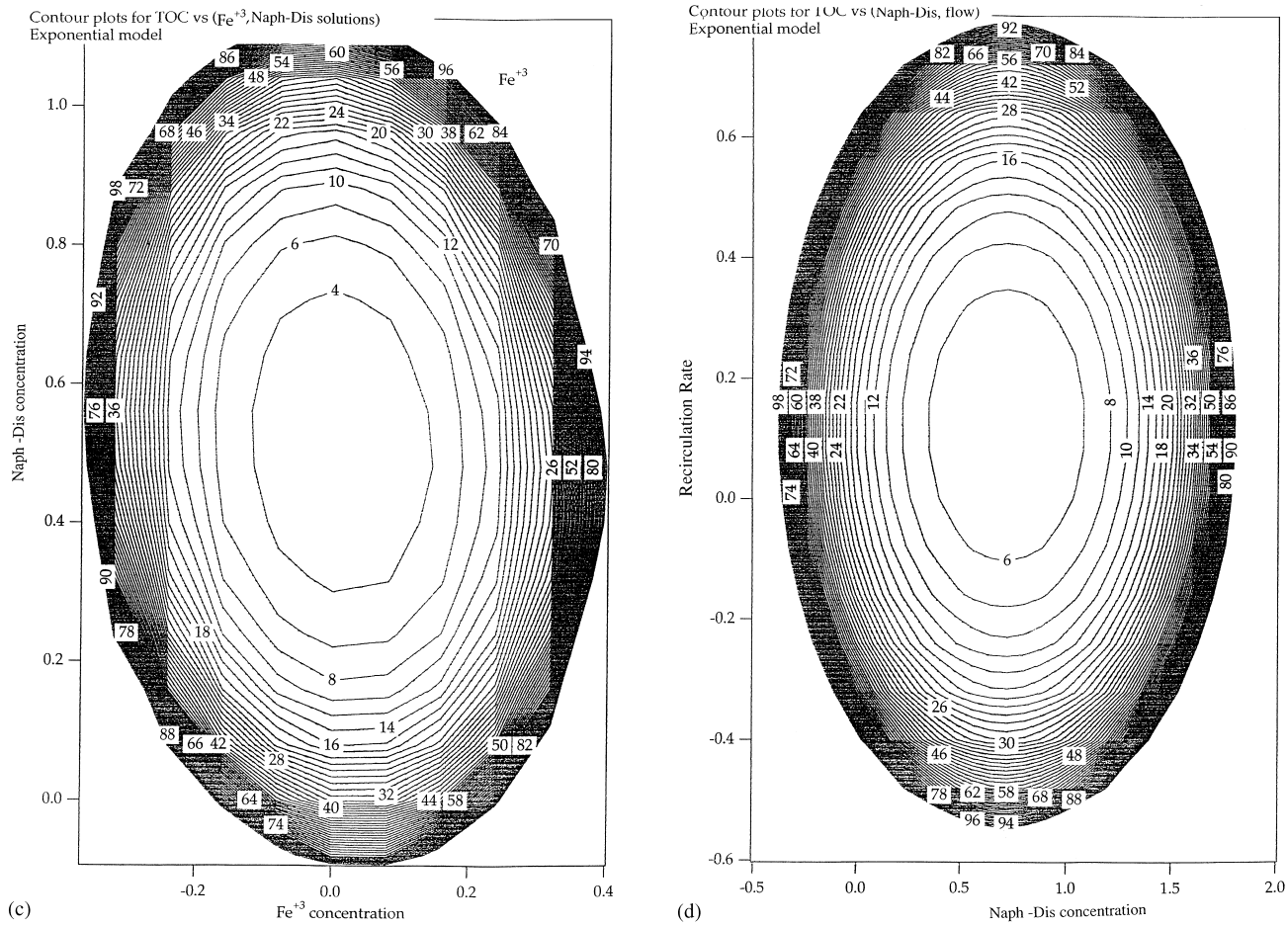

Fig. 8. (*Continued*)

Contour plots were obtained using the IGOR 3.0 Program in Power Macintosh 8200 / 120 [34]. The regions for the minima of Z values have been located as a function of the combinations of variables taken in pair Eq. (13). The variation of TOC vs. H_2O_2, Fe^{3+} is shown in Fig. 8(a). Similar contour plots can be drawn for TOC vs. H_2O_2, concentration of Naph-Dis and TOC vs. Fe^{3+}, concentration of Naph-Dis and TOC vs. Naph-Dis, recirculation rate, respectively in Fig. 8(b)–(d). These plots were obtained by calculating the coefficients of the exponential function Eq. (13) and drawing subsequently the contour for the respective pair of variables. The central regions for the three contours plots indicate the minimum value for the function Z(TOC). Fig. 8(a) shows that the inlet TOC (mg C l^{-1}) decreases from 98 to final TOC of 8 mg l^{-1}. The time variable has been fixed at 2 h (Figs. 2–6). This is an implicit variable in the experimental results presented in Figs. 8–10.

The purpose of Fig. 9(a) and (b) is to find the region in which the TOC is a minimum as a function of three experimental variable as opposed to two variables shown in Fig. 8(a)–(d). Fig. 9(a) shows the overlap of the contour plots of TOC vs. H_2O_2, recirculation rate and Naph-Dis concentration and Fig. 9(b) shows TOC vs. H_2O_2, Fe^{3+} and Naph-Dis concentration. The overlap of the minima of the contour plots to find the lowest Z(TOC) is seen in Fig. 9(a) and (b) through a three-variable representation in two dimensions using double vertical axes. The central regions at the four contours plots indicate four regions in which the TOC attained a minima. The central regions in Fig. 9(a) and (b) represent a degradation close to 98%, since the residual 2% of the initial TOC is the limit for the model used. Therefore, the exponential function allowed to predict the optimal conditions for the TOC decrease up to almost complete TOC abatement in solution. The dotted lines in Fig. 3 show the calculated values from the exponential model by way of Eq. (13). The experimental results are shown by full lines in Fig. 3. The predictive value of Eq. (13) is tested in this way. Each dotted line corresponds to the different values of added H_2O_2 as indicated in the caption to Fig. 3. The value of the adjustable parameters in Eq. (13) is obtained by fitting the initial and final TOC values. Each value of TOC can be calculated in Eq. (13) by way of the coefficients b_o, b_1, b_2, b_{11}, b_{12}, and b_{22}. The ensemble was obtained from the 2D contour plots in Fig. 8. These values implicitly contained the variable (2 h). The following relation is used

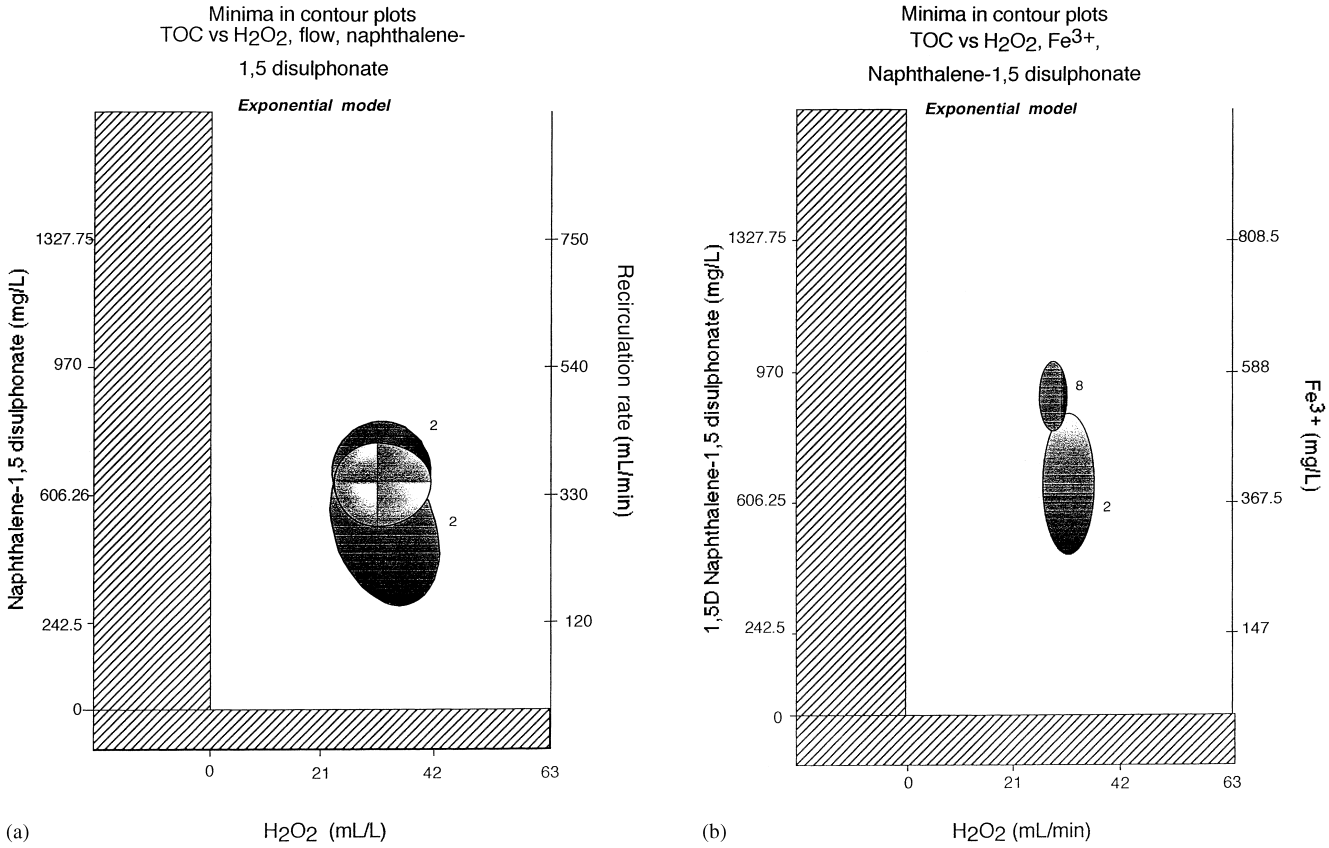

Fig. 9. Minima regions for TOC as a function of three parameters obtained by the overlap of the contour plots with the lowest TOC values for (a) TOC (Z function) vs. Naph-Dis, H_2O_2 and Fe^{3+} and (b) TOC (Z function) vs. Naph-Dis, H_2O_2 and recirculation flow rate.

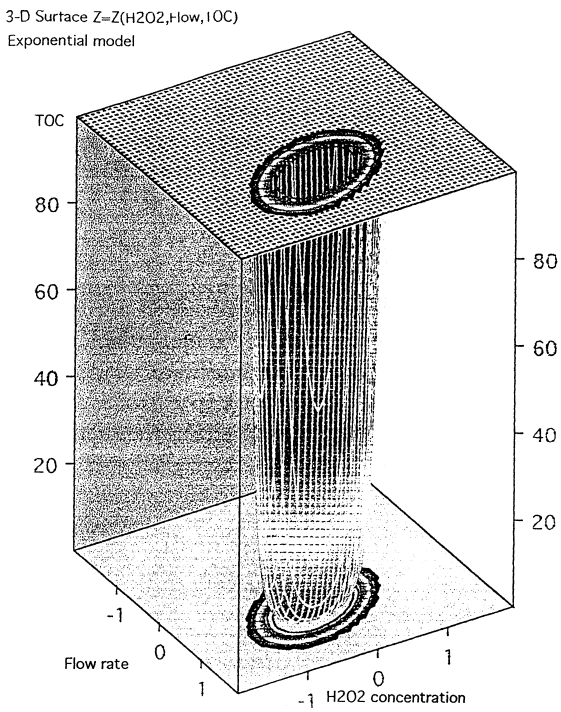

Fig. 10. 3D surface plots from the exponential function for TOC vs. H_2O_2 and the recirculation flow rate showing the 2D planes inside the cube.

$$Z(\mathrm{TOC}) = 31.1\exp(-15.98x_1 - 13.97x_2 + 18.98x_1^2 + 117.43x_2^2 + 3.26x_1x_2) \quad (14)$$

to fit the experimental data. The values of x_i, x_i^2 and x_ix_j correspond to the experimental values at any time between 0 and 120 min for any of the solution parameters chosen to optimize Z(TOC) in Eq. (14). The value of x_i relates to the amount of H_2O_2 (in ml min^{-1}) or Fe^{3+} (mg l^{-1}) present during this time interval in the solution (Fig. 8(a)). That is, the real variable u is given by the expression $x_i = (u_i - u_{io})/\Delta u_i$, where u_{io} is the value of u_i at the center of the experimental region and $\Delta_{ui} = (u_{imax} - u_{imin})/2$. For example, at $t = 20$ min, H_2O_2 has been added at the rate of 150 ml min^{-1} l^{-1}, the amount of H_2O_2 in solution is 3 ml l^{-1}. As $u_{io} = 0$, and the range of variation goes from 0 to 18 ml l^{-1} (120 min × 150 μl min^{-1} l^{-1}), $x_i = (3 - 0)/9 = 1/3$. The value of x_2 relates to u_2 (the Fe^{3+} ion concentration) and this value is a constant as the Fe ions are only added at the beginning of the reaction. The product of x_1x_2 will vary according to x_1 with time since x_2 stays a constant during the treatment. The dotted lines in Fig. 3 show the calculated values for the experimental model for the different amounts of H_2O_2 added during the reaction according to (Eq. (14)). The experimental and calculated values agree within 95% or better confirming the validity of the model used.

Fig. 10 show the 3D surfaces variation of TOC vs. H_2O_2, flow rate. In the top and bottom faces of each cube the contours plots are seen which were presented previously in Fig. 8(a)–(d). Such projections help to visualize the complex relation among the variables affecting the photodegradation. Time is again the implicit parameter in 3D surfaces presented in Fig. 10.

4. Conclusions

The parameters affecting the kinetics and efficiency of the photo-assisted oxidation of naphthalene 1,5-disulphonate have been reported and modeled in a photoreactor. The removal of long-lived micropollutants in relatively short times is shown to be possible under mild conditions and at room temperature using low energy light. The oxidation with H_2O_2 alone in the dark and under light was seen to be much less effective than when iron and copper salts were added in conjunction with H_2O_2. The efficiency of oxidation was limited by the absorption of light by the Fe ion charge transfer band in the solution. This latter species (and their complexes in solution) was the photoactive chromophore of the pollutant degradation. During the experimental work, it was observed that the experimental curves of the TOC vs. time for the chemical parameters affecting the degradation followed a near exponential form. The modeling proposed in this study allows a rigorous approach when minimizing the time, energy, chemicals, pH and overall cost for the abatement of Naph-Dis in solution. The modelization allowed the optimal conditions for the substrate and the intermediates generated in solution up to 2% of the initial C-content in the solution. The energy term is of particular importance since it refers to the use of expensive photons which should only be used for the shortest time to achieve biocompatibility for Naph-Dis in solution. In this way it is possible to determine the most suitable timing for further degradation by low cost bacterial degradation in a waste-water treating facility.

Acknowledgements

This work was supported by the European Communities Environmental Program ENV-CT 95–0064 (OFES Contract No. 96.0350, Bern)

References

[1] W. Giger, Th. Polger Altenbach, International Environmental Technology Guide, vol. 45, 1993.
[2] S. Shullerer, H. Brauch, F. Fimmel, Vom Wasser 75 (1990) 83.
[3] M. Halmann, Photodegradation of Water Pollutants, CRC Press, Boca Raton, FL, 1996.
[4] P. Pitter, J. Chudoba, Biodegradability of Organic Substances in the Aquatic Environment, CRC Press, Boca Raton, FL, 1990.
[5] H. Roques, Chemical Water Pretreatment, Wiley, Weinheim, 1996.
[6] T.R. Crompton, Toxicants in the Aqueous Ecosystem, Wiley, Weinheim, 1997.
[7] G. Chaudri, G. Biol, Degrad. Biochem. Toxic Chem, Dioscorides Press, Portland, Oregon, 1994, pp. 169–182.
[8] T. Ohe, Y. Watanabe, Agric. Biol. Chem. 52 (1988) 2409.
[9] C. Canalis, D. Hempel, Wasser, Abwasser. 113 (1929) 226.
[10] B. Bashan, K. Haberer, Th. Knepper, Vom Wasser. 84 (1995) 369.
[11] E. Gilbert, Water Res. 21 (1987) 1273.
[12] M. Kimura, Y. Ogata, Chem. Soc. Jpn. 51 (1983) 471.
[13] A. Neilson, Organic Chemicals in the Aquatic Environment, Lewis Publications, Boca Raton, FL, 1985.
[14] F.D. Ollis, H. Al-Ekabi, Photocatalytic Purification and Treatment of Water and Air, Elsevier, Amsterdam, The Netherlands, 1993.
[15] J. Bandara, C. Pulgarin, P. Peringer, J. Kiwi, J. Photochem. Photobiol. A 111 (1997) 253.
[16] P.J. Scott, F.D. Ollis, Environ. Progr. 14 (1994) 88.
[17] A. Cassano, C. Martin, R. Brandi, O. Alfano, Ind. Eng. Chem. Res. 34 (1995) 2155.
[18] A. Vogelpohl (Ed.), Int. Conf. on Oxidation Technologies for Water and Waste Water Treatment, 12–15 May, Goslar, Germany, 1995.
[19] H. Al-Ekabi, Proc. 4th Int. Conf. on Advanced Oxidation Technologies for Water and Air Remediation, Abstracts, Orlando, FL, 1997.
[20] G. Heller, H. Langan, Chem. Soc. Perkin. Trans. 2 (1981) 341.
[21] Ch. Walling, Acc. Chem. Res. 8 (1975) 125.
[22] J. Bandara, J. Kiwi, C. Pulgarin, Environ. Sci. Technol. 30 (1996) 1261.
[23] J. Bandara, J. Kiwi, G-M. Pajonk, J. Mol. Cat. A. 111 (1996) 333.
[24] B. Faust, J. Hoigné, J. Atoms. Environ. 24 (1990) 79.
[25] R. Knight, R. Sylva, J. Inorg. Nuc. Chem. 37 (1975) 779.
[26] V. Balzani, V. Carassiti, Photochemistry of Coordination Compounds, chap. 10, Academic Press, London, 1970, p. 145.
[27] J. Weiss, Naturwiss. 23 (1935) 64.
[28] M.A. Fox, C. Chen, J. Younathan, J. Org. Chem. 49 (1969) 1984.
[29] J. Theurich, D. Bahnemann, R. Vogel, I. Rajab, Res. Chem. Intermed. 23 (1997) 247.
[30] R. Atkinson, J. Phys. Chem. Ref. Data 20 (1991) 459.
[31] G. Box, P. Hunter, J. Hunter, Statistics for Experimenters: An Introduction to Design, Data Analysis and Model Building, Wiley, New York, 1978.
[32] A. Khuri, J. Cornell, Response Surfaces, Design and Analyses, Marcel Dekker, New York, 1987.
[33] E. Balanosky, J. Kiwi, Ind. Eng. Chem. Res. 37 (1998) 347.
[34] The use of Wavemetrics Program IGOR 3.0 (1997) with a power Macintosh 8200 / 120 allowed calculation of the contour plots and the 2D and 3D surfaces shown in the text.